Journal Pre-proof

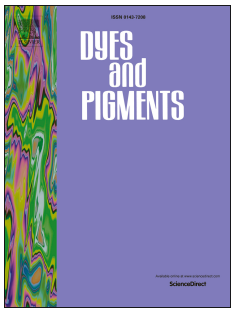

The development of coumarin Schiff base system applied as highly selective fluorescent/colorimetric probes for Cu^{2+} and tumor biomarker glutathione detection

Zhi-Gang Wang, Xiao-Jing Ding, Yu-Ying Huang, Xiao-Jing Yan, Bin Ding, Qing-Zhong Li, Cheng-Zhi Xie, Jing-Yuan Xu

PII: S0143-7208(19)32744-5

DOI: https://doi.org/10.1016/j.dyepig.2019.108156

Reference: DYPI 108156

To appear in: *Dyes and Pigments*

Received Date: 27 November 2019

Revised Date: 18 December 2019

Accepted Date: 18 December 2019

Please cite this article as: Wang Z-G, Ding X-J, Huang Y-Y, Yan X-J, Ding B, Li Q-Z, Xie C-Z, Xu J-Y, The development of coumarin Schiff base system applied as highly selective fluorescent/colorimetric probes for Cu^{2+} and tumor biomarker glutathione detection, *Dyes and Pigments* (2020), doi: https://doi.org/10.1016/j.dyepig.2019.108156.

Author Statement

Zhi-Gang Wang: Investigation, Validation, Writing - Original Draft

Xiao-Jing Ding: Validation, Formal analysis, Resources

Yu-Ying Huang: Formal analysis, Writing - Review & Editing

Xiao-Jing Yan: Data Curation, Software

Bin Ding: Writing - Review & Editing, Funding acquisition

Qing-Zhong Li: Software

Cheng-Zhi Xie: Conceptualization, Methodology, Writing - Review & Editing

Jing-Yuan Xu: Conceptualization, Supervision, Funding acquisition

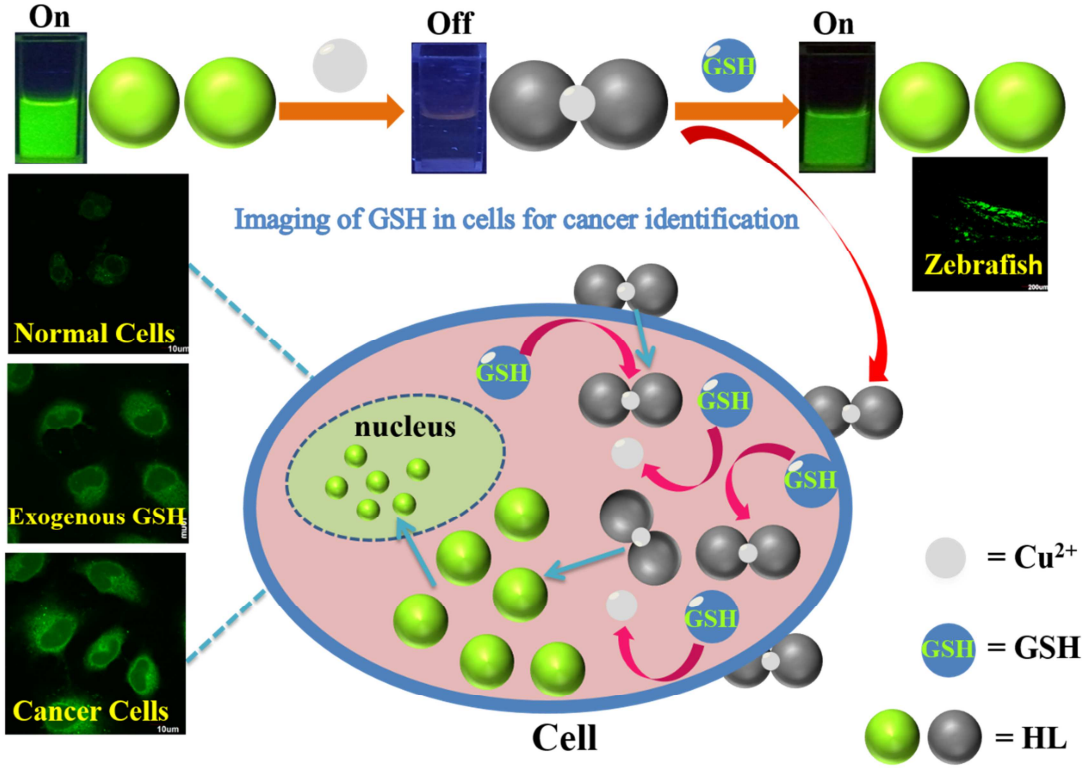

A highly selective fluorescent/colorimetric probe system for detecting Cu^{2+} and tumor biomarker glutathione.

The development of coumarin Schiff base system applied as highly selective fluorescent/colorimetric probes for Cu^{2+} and tumor biomarker glutathione detection

Zhi-Gang Wang[a,1], Xiao-Jing Ding[a,1], Yu-Ying Huang[a], Xiao-Jing Yan[a], Bin Ding[b,c], Qing-Zhong Li[d], Cheng-Zhi Xie[a,b,*], Jing-Yuan Xu[a,*]

[a]Tianjin Key Laboratory on Technologies Enabling Development of Clinical Therapeutics and Diagnostics, School of Pharmacy, Tianjin Medical University, Tianjin 300070, China.

[b]Key Laboratory of Advanced Energy Materials Chemistry (Ministry of Education), Nankai University, Tianjin 300071, China.

[c]College of Chemistry, Tianjin Normal University, Tianjin 300387, China.

[d]The Laboratory of Theoretical and Computational Chemistry, School of Chemistry and Chemical Engineering, Yantai University, Yantai 264005, China.

[1]These authors contributed equally.

Corresponding author. E-mail address: xujingyuan@tmu.edu.cn (J.-Y. Xu), xiechengzhi@tmu.edu.cn (C.-Z. Xie)

Abstract:

Overexpression of tumor biomarker glutathione (GSH) has been documented in numerous types of cancers, therefor GSH-activated light-up chemosensors for tumor identification require great attention. A new colorimetric/fluorescent probe (7-(diethylamino)-2-oxo-2H-chromen-3-yl)methylene)-4-(dimethylamino) benzohydrazide (HL) was prepared, which could be applied in discriminating Cu^{2+} and further recognizing GSH based on its Cu complex. Firstly, the probe HL toward Cu^{2+} exhibited selective fluorescence quenching and obvious color change from yellow to orange-red under visible light. Further, when GSH was introduced to the Cu^{2+}-2HL system, the fluorescence recovered rapidly due to the high affinity of GSH to Cu^{2+}, meanwhile the color reverted back to former yellow. Based on fluorescence titration, the detection limits were calculated as 2.40×10^{-8} M and 1.29×10^{-7} M for Cu^{2+} and GSH, respectively. The combination mode of HL with Cu^{2+} was investigated in detail by Job plots, ESI-MS, FT-IR, and DFT studies. Probes HL and Cu^{2+}-2HL showed relatively less toxicity and were employed for biological imaging in cells and zebrafish. Remarkably, the detection for endogenous GSH by this developed sensor platform implied great potential application prospect in cancer diagnosis.

Keywords: Fluorescent probe; “Naked-eye” detection; Glutathione monitoring; DFT calculation; Bioimaging; Cancer diagnosis

1. Introduction

Among the important metal ions in human body, copper plays pivotal roles in many biological processes [1]. Abnormality of Cu^{2+} in the human body may destroy normal physiological functions and cause cancer or neurodegenerative diseases [2–4]. Elevated copper were often found in various malignancies, which is the necessary angiogenic component in tumor growth and metastasis [5,6]. Meanwhile, Cu^{2+} is also considered to be one of environmental pollutants, for which the World Health Organization has stipulated the value of Cu^{2+} in drinking water below 2 ppm [7]. On the other hand, thiols, such as glutathione (GSH), cysteine (Cys), and homocysteine (Hcy), play the vital roles in maintaining biological redox homeostasis of bodies and issues [8,9]. As the most abundant nonprotein thiol, GSH is an essential redox control agent to resist against free radicals and toxins, and also act as biomarker for various medical diagnoses [10]. Abnormal levels of GSH is associated with cancer, Alzheimer’s disease, AIDS, liver damage, and other ailments [11,12]. In comparison with normal tissues, tumors always express higher levels of GSH, which could be used to differentiate cancer and normal cell [13,14]. Detection and imaging of tumor biomarker GSH will greatly improve the diagnosis of cancer patients in the early stages and contribute to precision cancer therapy [15–17]. Hence, it is very necessary to develop efficient methods for Cu^{2+} and GSH detection in biosystem, especially for

cancer diagnosis.

Fluorescent and colorimetric chemosensors for metal ions and cancer biomaker have received considerable attention in recent years for their high selectivity, sensitivity, simplicity and fast response [18–22]. Owning to the outer electronic arrangement ($3d^9$) of Cu^{2+} and its strong binding affinity toward thiols, copper complexes were successfully used to detect thiols through measuring changes in fluorescence intensity or UV-vis absorption [23–26]. The chemosensors can specifically distinguish Cu^{2+}, then generated non-emissive fluorophore-Cu(II) complexes could further recognize thiols by displacement processes. Although this method is simple and convenient, it is often limited by lower sensitivity, no visual sensing and high toxicity.

It is well known that the key element of probe design is the exquisite combination of different functional groups with appropriate properties. Coumarin dye is extensively used as building block and chromosphere in designing fluorescent probe owning to its well-biocompatibility, good light stability, visible emission wavelength, high fluorescence sensitivity and readily modified backbone [27–30]. Simultaneously, acylhydrazine Schiff base derivatives have good applications in the fields of medicine and sensor, which can provide special coordination environment and exhibited low toxicity as well as good water solubility [31–35]. Considering these aspects, we designed a new chemosensor (7-(diethylamino)-2-oxo-2H-chromen-3-yl)methylene)-4-(dimethylamino)benzohydrazide (HL) to detect Cu^{2+} and GSH by “on-off-on” fluorescent switch strategy

accompanied with obvious colorimetric responses in neutral aqueous media, which possess high sensitivity and excellent selectivity over a wide range of ions and amino acids. Furthermore, the developed sensor platform could be successfully applied in biological imaging and medical diagnostics with satisfied results.

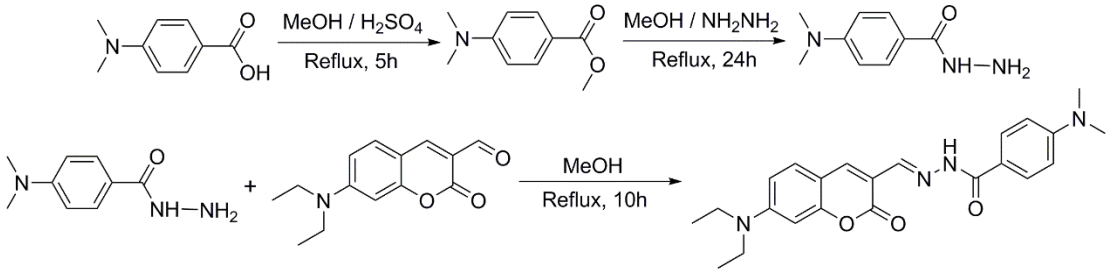

Scheme 1. Syntheses of probe HL.

2. Experimental section

2.1. Materials and instruments

All chemicals were obtained from commercial providers and used without purification. Zebrafish embryos and larvae were purchased from Nanjing EzeRinka Biotechnology Co., Ltd. ^{1}H-NMR and ^{13}C-NMR spectra were obtained on Bruker AVANCE III spectrometer. FT-IR spectra were measured on NICOLET IS50 FT-IR spectrometer. UV-vis absorption spectroscopies were recorded on JASCO V-770 spectrometer. Fluorescence measurements were acquired on Hitachi F-7000 fluorescence spectrophotometer. Electrospray ionization mass spectrometries (ESI-MS) were carried out on Finnigan LCQ electron spray mass spectrograph. Images were performed by confocal fluorescence microscope (Olympus FV1000, Japan). The copper contents was also determined by inductively-coupled plasma mass

spectrometry (ICP-MS, Optima 5300DV, PerkinElmer, USA). Steady-state fluorescence experiment was performed on Edinburgh FS5 spectrofluorometer.

2.2. Preparation of HL

The synthesis procedure of HL was shown in Scheme 1. First of all, 4-dimethylaminobenzhydrazide [36] and 7-diethylaminocoumarine-3-aldehyde [37] were synthesized followed to the reported methods. Then to a solution of 4-dimethylaminobenzhydrazide (89.6 mg, 0.5 mmol) in 25 mL anhydrous methanol, 7-diethylaminocoumarine-3-aldehyde (122.7 mg, 0.5 mmol) in 15 mL anhydrous methanol was added slowly under stirring. The mixture was refluxed for 10 h at 80 ^{o}C. The resulting solution was cooled to room temperature, and the precipitate was filtered, washed with methanol twice and dried under vacuum. Finally, 124 mg orange solid of (7-(diethylamino)-2-oxo-2H-chromen-3-yl)methylene)-4-(dimethylamino)benzohydrazide (HL) was obtained at 61% yield. ^{1}H NMR (400 MHz, DMSO-d_6): δ (ppm): 11.62 (s, 1H, NH), 8.47 (s, 1H, CH=N), 8.33 (s, 1H, ArCH), 7.82 (d, J = 8.9 Hz, 2H, ArCH), 7.64 (d, J = 9.0 Hz, 1H, ArCH), 6.78 (d, J = 2.4 Hz, 1H, ArCH), 6.75 (d, J = 9.0 Hz, 2H, ArCH), 6.59 (s, 1H, ArCH), 3.47 (q, J = 7.0 Hz, 4H, CH_2), 3.00 (s, 6H, CH_3), 1.14 (t, J = 7.0 Hz, 6H, CH_3) (Fig. S1). ^{13}C NMR (101 MHz, DMSO-d_6) δ (ppm): 160.88, 156.35, 151.13, 151.11, 148.23, 137.99, 130.69, 129.09, 119.37, 116.85, 113.01, 110.79, 109.65, 108.08, 96.38, 44.19, 40.94, 12.34 (Fig. S2). ESI-MS (*m/z*) calculated $[HL + H]^+$ = 407.2078, found 407.2077, $[HL + Na]^+$ = 429.1897, found

429.1897(Fig. S3). FT-IR (KBr, cm^{-1}): υ(hydrazide N–H): 3304.43, υ(coumarin C=O): 1696.40, υ(hydrazine C=O): 1651.52, υ(Schiff-base C=N): 1615.94.

2.3. Absorbance and fluorescence measurements

HL was dissolved in *N*,*N*-dimethylformamide to make a stock solution with concentration of 10^{-3} M. All metal ion stock solutions were prepared from their corresponding nitrate salts with methanol, meanwhile all anion stock solutions were prepared from their corresponding sodium salts with methanol. Amino acid stock solutions were prepared using double distilled water. All the stock solutions (10^{-3} M) were diluted properly for the spectrometry measurements. Job plots analysis was performed by using UV-vis absorption spectrum, in which the proportions of HL and Cu^{2+} varied meanwhile the total concentration of HL and Cu^{2+} remained unchanged. The solution of copper complex (Cu^{2+}-2HL) for the detection of GSH were prepared *in situ* by adding 10^{-3} M $Cu(NO_3)_2$ (20 μL) to 20 μM HL solution (2 mL), which could be diluted to other concentrations.

2.4. Toxicity and bio-imaging studies

MCF-7 (breast carcinoma cells) and HUVEC (human umbilical vein endothelial cell) were obtained from American. The toxicity study of probe HL and its Cu complex were determined by MTT assay. MCF-7 cells were cultured on 96-well cell-culture plates at a density of 3×10^3 cells/well, and incubated at 37 ^oC. 24 h later, the cells were incubated with HL and Cu^{2+}-2HL with varied concentrations for 6 h. Then 10 μL MTT solution was added and incubated for another 4 h. Finally, the

supernatant was removed and 100 μL DMSO was added to dissolve the formed formazan precipitate before measurements on the Infinite® 200 Pro NanoQuant Microplate Reader.

The cancerous cells MCF-7 and normal cells HUVEC were trypsinised and reseeded at 37 °C. 12 h later, they were incubated with 10 μM Cu^{2+}-2HL or HL for 30 min. GSH, *N*-ethylmaleimide (NEM) or $Cu(NO_3)_2$ with different concentration was loaded selectively for another 30 min. After washing cells with cold PBS two times, fluorescence images were taken.

Zebrafish embryos and larvae (3-day-old) were incubated with Cu^{2+}-2HL solution (10 μM) for 1 h, then washed with deionized water three times to remove excess Cu^{2+}-2HL. Fluorescence images of zebrafish embryos and larvae were conducted by using confocal laser scanning microscope. For comparison, zebrafish larvae were pretreated with 50 μM NEM for 30 min to block thios, then incubated with Cu^{2+}-2HL and carried fluorescence imaging under the same condition.

3. Results and discussion

3.1. Colorimetric sensing studies

The absorption spectra of HL with various metal ions were measured in CH_3OH/H_2O (v/v = 1/1) solution (PBS buffer, pH = 7.4). As shown in Fig. S4, the HL exhibited a strong broad absorption peak at 454 nm, while upon addition of Cu^{2+}, the maximum absorption peak was red-shifted to 487 nm. The response time was below 1 minute. The absorption band with other metal ions were almost unchanged except Ni^{2+}, for which the maximum absorption slightly shifted to long-wave band ($\Delta\lambda$ is

about 10 nm). In addition, all the tested metal ions didn't cause apparent interference on absorption spectra of the HL-Cu^{2+} system (Fig. S5), which is favorite to the colorimetric detection of Cu^{2+} under complicated environment. The absorption titration experiments have been further performed. As shown in Fig. 1a, with increasing concentrations of Cu^{2+}, the maximal peak at 454 nm gradually decreased and a new peak increased at 487 nm concurrently with two well-defined isosbestic points at 389 and 470 nm, revealing that only one complex formed from HL and Cu^{2+} [38]. The Cu^{2+}-2HL system was prepared by adding 0.5 equiv. Cu^{2+} to the solution of HL to act as a new probe for GSH. When GSH was added to the Cu^{2+}-2HL system, the maximum absorption peak at 487 nm was blue-shifted to 454 nm again (Fig. 1b). Both of the above absorption titration displayed good linear relationship between the absorbance and Cu^{2+}/GSH concentrations (within the range of 0–10 μM for Cu^{2+} and 0–25 μM for GSH) (Figs. S6, S7 and Fig. 1 insert). It was found that detection limits (DL) were 1.23×10^{-7} M for Cu^{2+} and 2.18×10^{-6} M for GSH. Details for DL calculations were shown in SI, Figs. S6 and S7.

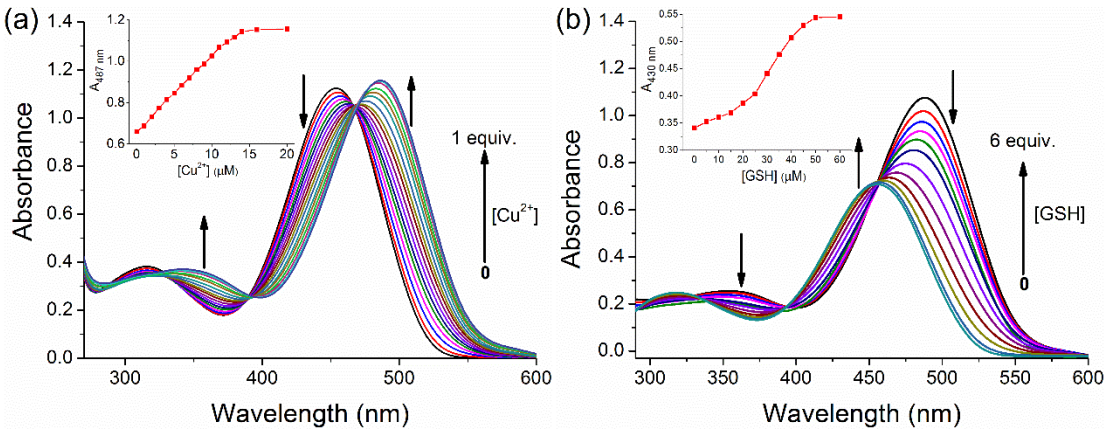

Fig. 1. Absorption titration spectra of (a) probe HL (20 μM) with increasing concentration of Cu^{2+}

(0–1 equiv.) and (b) probe Cu^{2+}-2HL (10 μM) with increasing concentration of GSH (0–6 equiv.) in CH_3OH-H_2O buffer solution. Inset: (a) the absorbance at 487 nm versus [Cu^{2+}]; (b) the absorbance at 430 nm versus [GSH].

3.2. Fluorescence sensing studies

The fluorometric analysis of probe system were determined in CH_3OH/H_2O (v/v = 1/1) PBS buffer solution (pH = 7.4) upon excitation at 450 nm. Probe HL can emit intense fluorescence at about 521 nm, which could be markedly quenched by the addition of Cu^{2+} due to the paramagnetic quenching effect [39] (Fig. 2a). For other metal ions (1 equiv. Na^+, K^+, Ca^{2+}, Mg^{2+}, Al^{3+}, Co^{2+}, Ni^{2+}, Fe^{3+}, Zn^{2+} and Cd^{2+}), most of them did not cause obvious changes except for Ni^{2+}. The fluorescence intensity for Ni^{2+} decreased by 11.9% in comparison with HL alone, while the quenching rate for Cu^{2+} reached to 89.8%. The excellent selectivity under complex condition is an important factor for practical application of fluorescence probe. To study the anti-interference property of probe HL, we conducted fluorescence experiments towards Cu^{2+} along with other ions. As shown in Fig. S8, most competing ions didn't significantly interfere the quenching effect of Cu^{2+} for probe HL. Notably, the existence of superfluous Na^+, K^+, Mg^{2+} and Ca^{2+} (which are important elements in biological activities) hardly perturbed the fluorescence of Cu^{2+}-HL system.

The obtained Cu^{2+}-2HL system could consequently act as a promising probe for fluorescence "off-on" detection of GSH *via* Cu^{2+} displacement approach. To evaluate the selectivity of fluorescence probe Cu^{2+}-2HL for GSH, the response of Cu^{2+}-2HL

(10 μM) to various amino acids including Arg, Asp, Cys, Glu, Gly, GSH, His, Iso, Lys, Met, Pro, Ser, Thr, Tyr and Val, as well as various anions (F^-, Cl^-, Br^-, NO_2^-, NO_3^-, HPO_4^{2-}, $H_2PO_4^-$, CH_3COO^-, $HS^-$and HSO_3^-) were measured, respectively. As shown in Fig. 2b and Fig. S9, the fluorescence emission at 521 nm significantly enhanced by about 9.2-fold with the addition of GSH, while other amino acids and anions exerted little influence on fluorescence emission. Additionally, competition experiments were also conducted (Figs. S10 and S11), in which other amino acids and anions did not seriously interfere with the measurement of GSH by probe Cu^{2+}-2HL, suggesting that Cu^{2+}-2HL had distinct potential to distinguish GSH in physiological environment.

Quantitative analysis of HL towards Cu^{2+}, as well as Cu^{2+}-2HL towards GSH, were both studied in detail by fluorescence titration experiment (Fig. 3). With the increase of Cu^{2+} concentrations (0–1 equiv.), the fluorescence intensity of HL was gradually reduced and reached a minimum when 0.6 equiv. of Cu^{2+} was introduced, while further increase of Cu^{2+} concentration did not cause significant change in the emission intensity. For Cu^{2+}-2HL system, corresponding enhancements of fluorescence intensity at 521 nm were followed with gradual addition of GSH. Excellent linear relationship between emission intensity and analytes (Cu^{2+} and GSH) were both observed in the low concentration region (For Cu^{2+}: 0–4 μM, for GSH: 0–10 μM; See insert of Fig. 3, Fig. S12 and Fig. S13), indicating that the chemosensor system could be used in quantitative determination of Cu^{2+} and GSH. The detection limits (DL) of probe HL for Cu^{2+} and Cu^{2+}-2HL for GSH were calculated to be

2.40×10^{-8} M and 1.29×10^{-7} M, respectively. Comparing with fluorescence detection method, the content of Cu^{2+} was also determined by ICP-MS, in which the relative error was below 5% (Table S1). In addition, according to the fluorescence titration results, the intrinsic binding constant K for Cu^{2+} with HL was determined to be 2.63×10^{5} M^{-1}, which was calculated by the Benesi-Hildebrand equation for 2:1 complex [9]. Details for DL and K calculations were displayed in SI and Fig. S14. Transient fluorescence titration experiment of Cu^{2+} has been performed. As shown in Fig. S15, the lifetime of Cu complex (τ = 0.29 ns) were obviously shorter than probe HL (τ = 0.49 ns), which was accordance with the fluorescence intensity changes. The quenching constants K_{SV} were determined as 3.77×10^{5} M^{-1} for Cu complex, according by the Stern–Volmer equation: $F_0/F = 1+ K_{SV}[Q]$ (Fig. S16) [40, 41]. And then, molecular quenching constants k_q for Cu complex was calculated to be 3.77×10^{13} $M^{-1}s^{-1}$ ($k_q = K_{SV}/\tau_0$, $\tau_0 = 10^{-8}$ s), which is much higher than the diffusion rate constant (*ca.* 10^{10} $M^{-1}s^{-1}$), thus assures the static quenching mechanism [42].

We know that most fluorescent probes are greatly affected by pH value, so we determined the fluorescence response of HL and Cu^{2+}-2HL from pH 2 to 12 (Fig. S17). The fluorescence intensity of HL and Cu^{2+}-2HL showed the similar trend and were stable in a broad pH range (4–12) except for a sharp downward trend from pH 3 to 4. Therefore, physiological pH value (7.4) was selected for experimental research, which is beneficial for GSH tracking in living system.

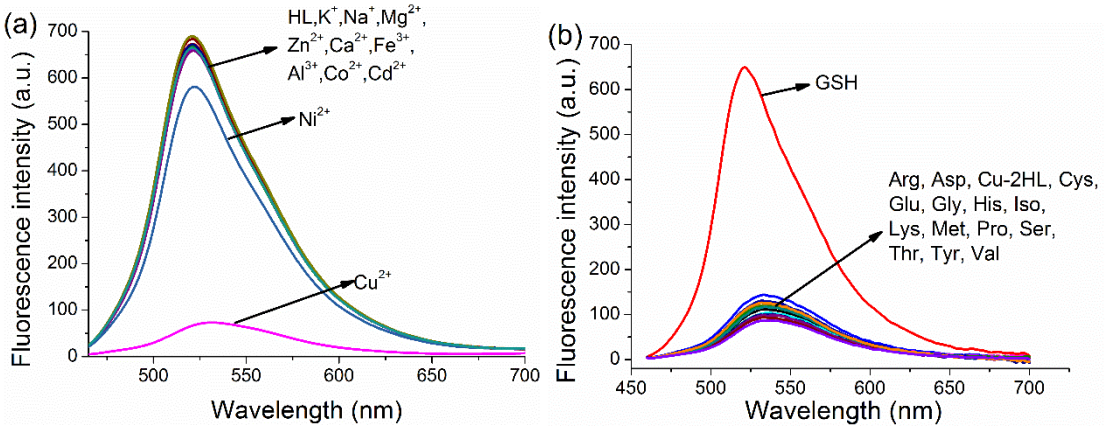

Fig. 2. The fluorescence emission spectra of (a) probe HL (10 μM) upon addition of 1 equiv. various metal ions and (b) Cu^{2+}-2HL (10 μM for HL, 5 μM for Cu^{2+}) upon addition of different amino acids (50 μM) in CH_3OH-H_2O buffer solution (λ_{ex} = 450 nm).

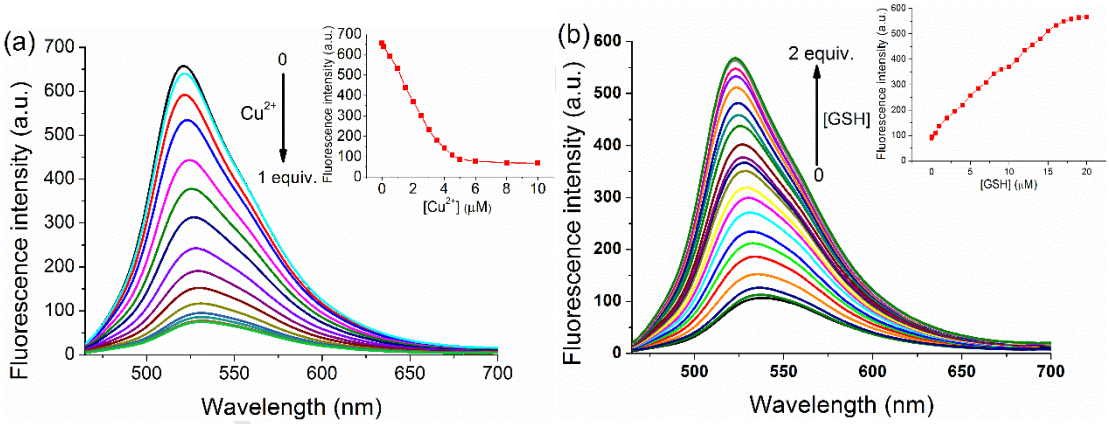

Fig. 3. The fluorescence titration spectra of (a) probe HL (10 μM) with increasing concentration of Cu^{2+} from 0 to 10 μM and (b) probe Cu^{2+}-2HL system (10 μM) with increasing concentration of GSH from 0 to 20 μM. Inset: the fluorescence intensity at 521 nm versus (a) [Cu^{2+}] and (b) [GSH] (λ_{ex} = 450 nm). The first points in titration experiments were set as 1×10^{-7} M and 2×10^{-7} M for (a) and (b), respectively .

3.3. "Naked-eye" detection

It should be noted that this chemosensor system has potential in "Naked-eye" detection for Cu^{2+} and GSH, which possess good practicability due to convenience

and easy-operation. As shown in Fig. 4, with addition of Cu^{2+}, the color of HL solution noticeably changed from yellow to orange-red, while no obvious response could be observed with other metal ions. Under 365 nm UV irradiation, probe HL exhibited green fluorescence. After adding Cu^{2+}, the green fluorescence disappeared, while no corresponding fluorescence changes occurred in the intervention of other surveyed metal ions. With addition of GSH, the color of Cu^{2+}-2HL system reverted back to former yellow, meanwhile displayed green fluorescence under 365 nm UV lamp (Fig. 5). Similarly, Color changes weren't disturbed by various amino acids. It is worth mentioning that all the response time for analytes were below 1 minute. Therefore, colorimetric probe HL and Cu^{2+}-2HL can quickly detect Cu^{2+} and GSH by visual observation, respectively.

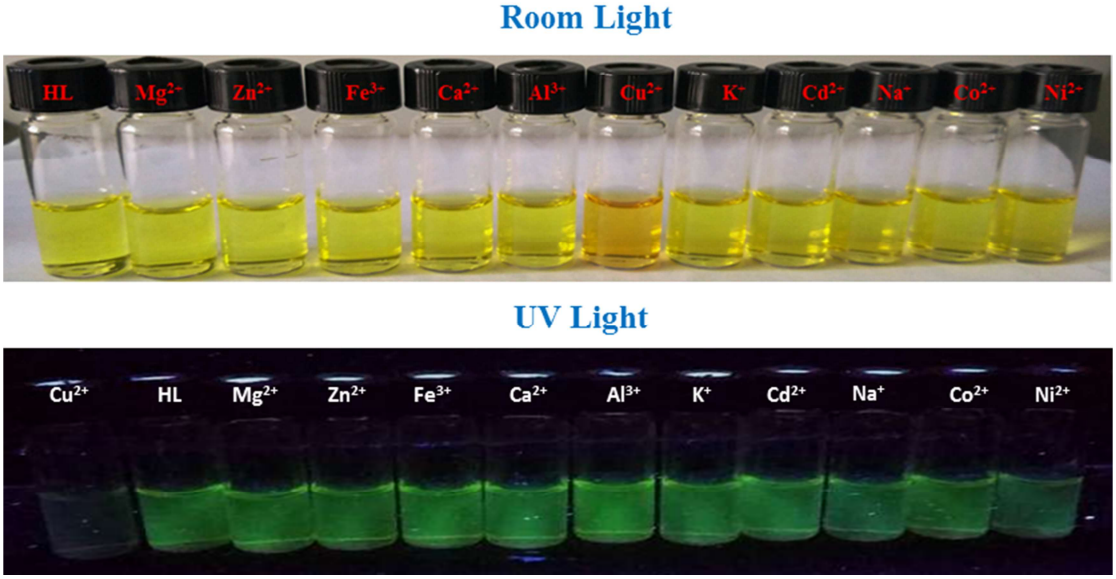

Fig. 4. The photograph of probe HL (10 μM) with visual color changes upon the addition of 1 equiv. of different metal ions in CH_3OH-H_2O buffer solution.

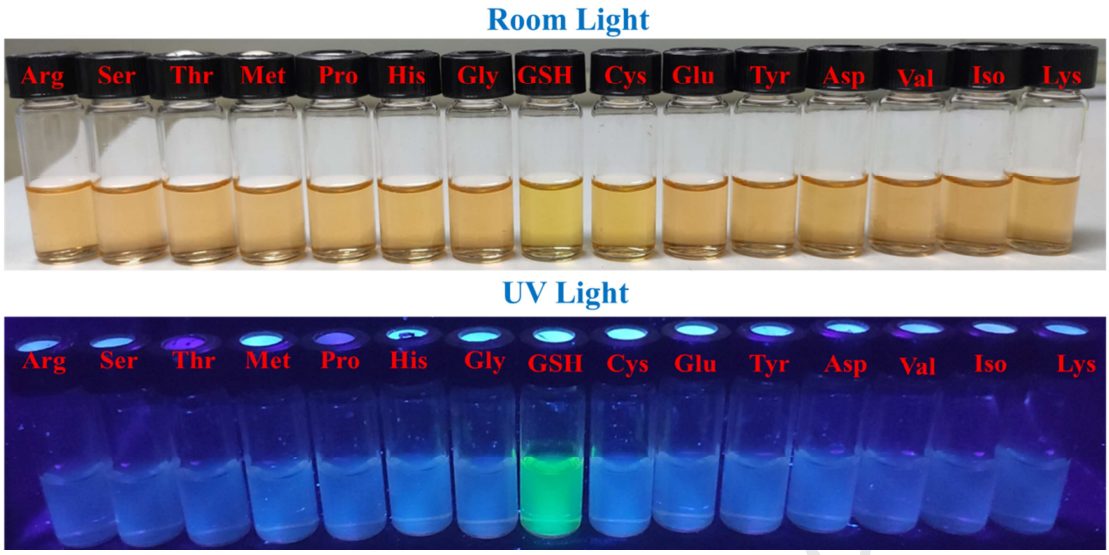

Fig. 5. The photograph of probe Cu^{2+}-2HL (10 μM for HL, 5 μM for Cu^{2+}) with visual color changes upon the addition of 1 equiv. of GSH and different amino acids.

3.4. Binding mode studies

For determining the binding stoichiometry of HL with Cu^{2+}, Job plots (Fig. S18) was obtained by absorption spectroscopy at 487 nm. The maximum absorption was obtained at Cu^{2+} molar fraction of ca. 0.33, which indicated the 2:1 combination ratio between HL and Cu^{2+}. ESI-MS experiment also proved the 2:1 binding stoichiometry between HL and Cu^{2+} (Fig. 6). The complex of HL with $Cu(NO_3)_2$ exhibited signal peak at m/z 874.3221, corresponding to $[CuL_2+H]^+$ (m/z: 874.3222). FT-IR spectroscopy provided more evidence for the binding of HL with Cu^{2+} (Figs. S19 and S20). For HL, strong characteristic bands at 1696.40, 1651.52 and 1615.94 cm^{-1} are attributed to ν(C=O, coumarin), ν(C=O, hydrazine) and ν(C=N), respectively. For complex, these bands weaken and red-shifted, which certified the binding of carbonyl and imino groups with metal ion [35].

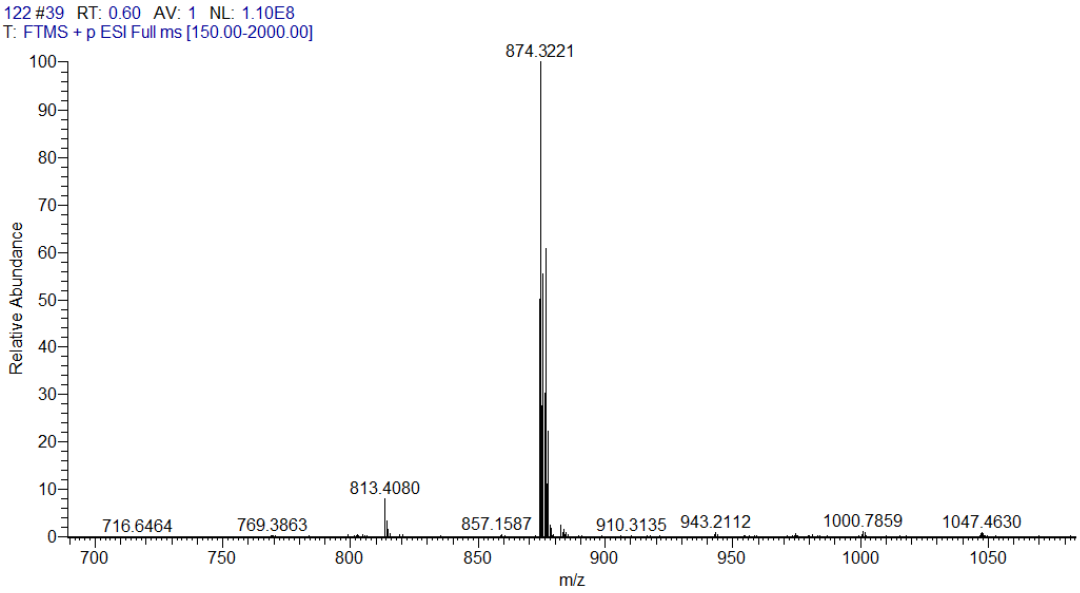

Fig. 6. The ESI-MS spectrum of Cu^{2+}-2HL.

Density functional theory (DFT) studies of HL and Cu complex were performed at the B3LYP level using Gaussian 09 programs [43]. The LANL2DZ basis set was used for Cu^{2+} whereas 6-31+G (d,p) for the other atoms. The optimized geometries of HL and Cu complex are presented in Fig. 7, which were both local minima in the potential energy surfaces without constrains of symmetry. For Cu complex, Cu^{2+} is located in a distorted octahedral environment with a CuN_2O_4 core involving imine nitrogen, hydrazide carbonyl oxygen and coumarin carbonyl oxygen from two tridentate L ligands. This coordination mode is consistent with the literature reported before [35,44,45]. The energy band gaps between HOMO (Highest Occupied Molecular Orbital) and LUMO (Lowest Unoccupied Molecular Orbital) are 3.357 eV for HL and 2.876 eV for Cu complex, respectively (Fig. S21), which is consistent with the red-shift effect of absorption peak [35].

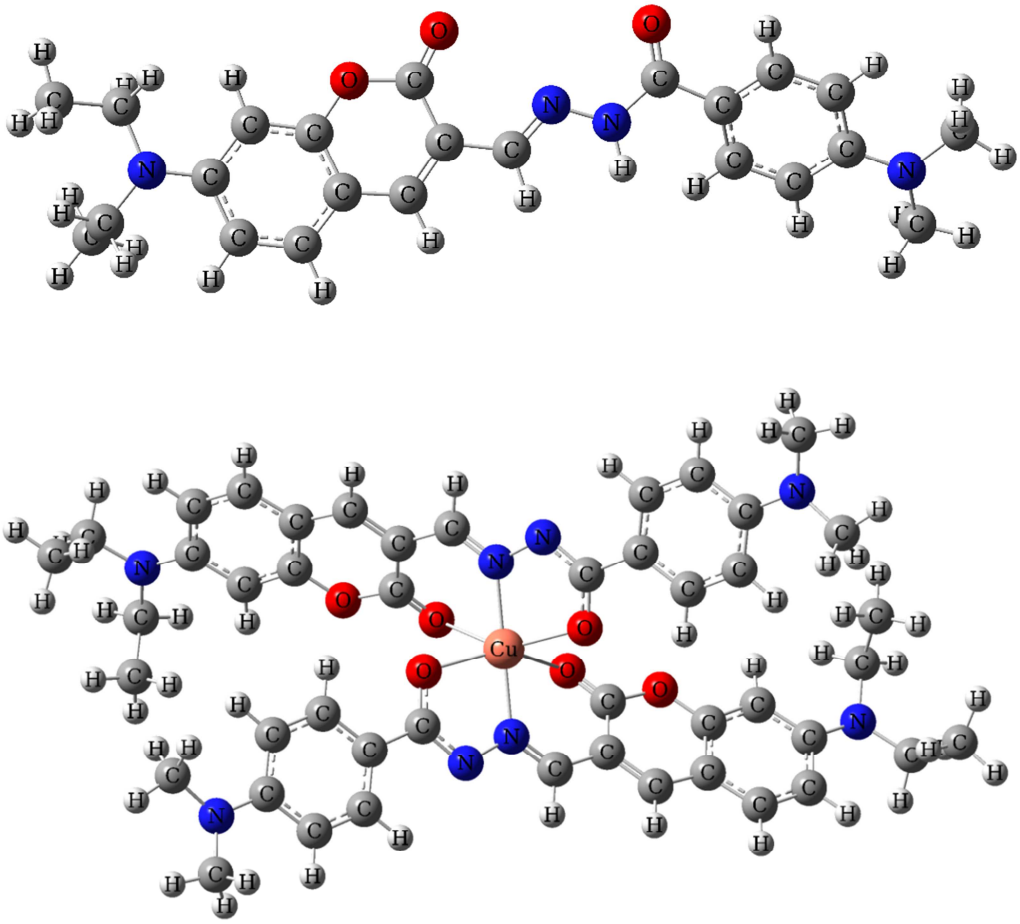

Fig. 7. Optimized structures of HL and its Cu complex.

3.5. GSH sensing in biological system

To further investigate the *in vivo* application of probe molecule, the cytotoxicities of HL and its Cu complex were investigated by MTT assay. MCF-7 cells were incubated with various concentrations of HL and Cu^{2+}-2HL for 6 h. As shown in Fig. 8, cell viability was higher than 95% over the full range of staining concentrations (0–100 μM) for HL and below 25 μM for Cu complex, which indicated that probe HL (10 μM) and Cu^{2+}-2HL (10 μM) could both be used safely for luminescence bio-imaging. It is generally believed that excessive copper ion is toxic to organisms, while the close encirclement by two chelated HL prevents the interaction of Cu^{2+} with

proteins, thus results in the low cytotoxicity of Cu^{2+}-2HL.

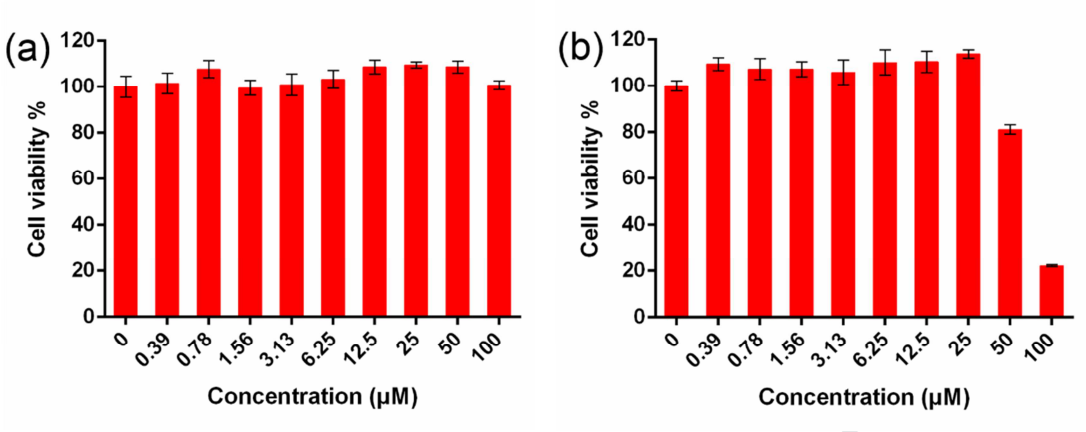

Fig. 8. Cell viability of MCF-7 cells after treatments with HL (a) and Cu^{2+}-2HL (b) for 6 h. Results are expressed as the mean ±S.D (n = 3).

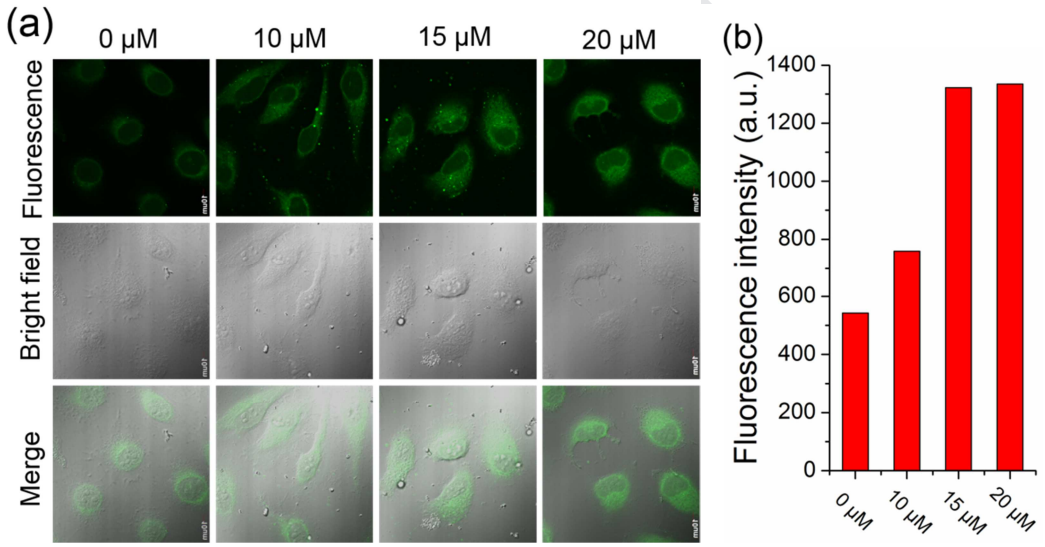

Fig. 9. (a) Confocal microscope images of MCF-7 cells which were incubated with indicated concentration of GSH followed by the treatment of probe Cu^{2+}-2HL (10 μM). Top: fluorescence images; middle: bright-field images; bottom: merged images. (b) Quantified fluorescence intensities of cells.

As shown in Fig. 9, after MCF-7 cells were incubated with 10 μM Cu^{2+}-2HL, significant fluorescence was observed and increased in a GSH dose-dependent way ([GSH] = 0–20 μM). The result suggested that probe Cu^{2+}-2HL was easily membrane

permeable and could detect GSH with high efficiency in live cells. Remarkably, obvious intracellular fluorescent emission was observed in MCF-7 cells even in the absence of exogenous GSH, which is attributed to the fact that GSH always maintains a high level in various cells. For confirming the fluorescence is caused by GSH, MCF-7 cells were pretreated with different concentration of NEM, which is an irreversible chelator of GSH, to consume endogenous GSH. Then MCF-7 cells were incubated with Cu^{2+}-2HL for another 30 min and imaged under microscopy. As shown in Fig. S22, the cellular fluorescence emission was effectively reduced by NEM in a dose-dependent way, which verified that probe Cu^{2+}-2HL could sensitively detect endogenous GSH. In addition, probe HL could detect excessive Cu^{2+} ions in MCF-7 cells through fluorescence quenching mechanism (Fig. S23).

Due to the importance of GSH level in tumor identification, we are interested in the detection capability of Cu^{2+}-2HL in differentiating endogenous GSH levels in tumor cells and normal cells. MCF-7 and HUVEC cells were both incubated with Cu^{2+}-2HL for 30 min then imaged under the same condition. It was found that the fluorescence intensity in MCF-7 cells was above 2-fold higher than that in HUVEC cells, suggesting higher GSH concentration in tumor cells (Fig. 10), which is consistent with the reports that high levels of GSH was generated in tumor cells for resisting intrinsic oxidative stress [46,47].

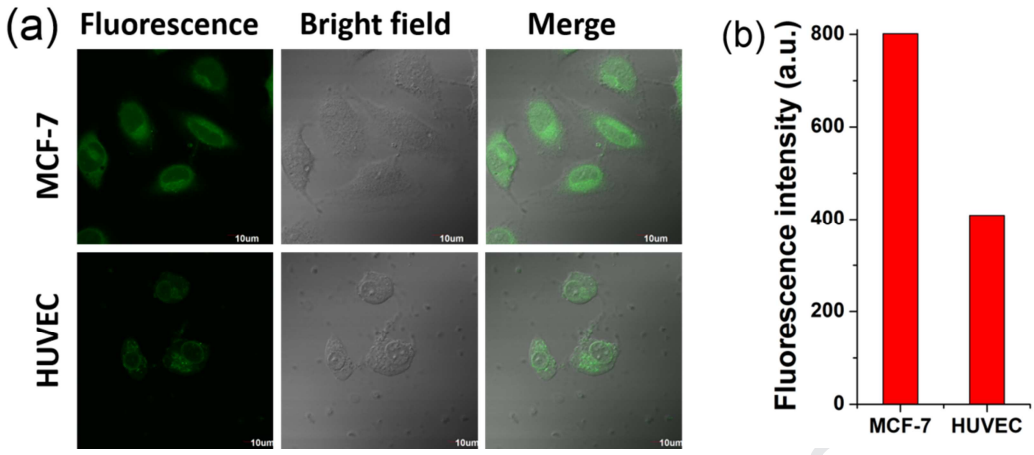

Fig. 10. (a) Comparison of endogenous GSH level in MCF-7 and HUVEC cells after incubation with fluorescent probe Cu^{2+}-2HL. Left: fluorescence images; middle: bright-field images; right: merged images. (b) Quantified fluorescence intensities of cells.

From a biological perspective, most human genes and zebrafish genes are homologous, and studies have proved that drug response of zebrafish has a high similarity with human being [48,49]. Due to the optical transparency, zebrafish are commonly selected as model animal for biomolecule detection in live organisms by fluorescence imaging. Therefore, the applicability of probe Cu^{2+}-2HL to trace GSH in zebrafish was investigated. Zebrafish larvae were incubated with 10 μM Cu^{2+}-2HL, resulting bright fluorescence signal in eyes and digestive system of zebrafish (Fig. 11 and Fig. S24). As reference experiment, when pre-treated zebrafish with 50 μM NEM, fluorescence was obviously weaken. In addition, The zebrafish embryos treated with 10 μM Cu^{2+}-2HL could also emit strong green fluorescence which scattered over the whole embryos (Fig. S25). All the above results indicated the potential extensive application of probe Cu^{2+}-2HL in living systems.

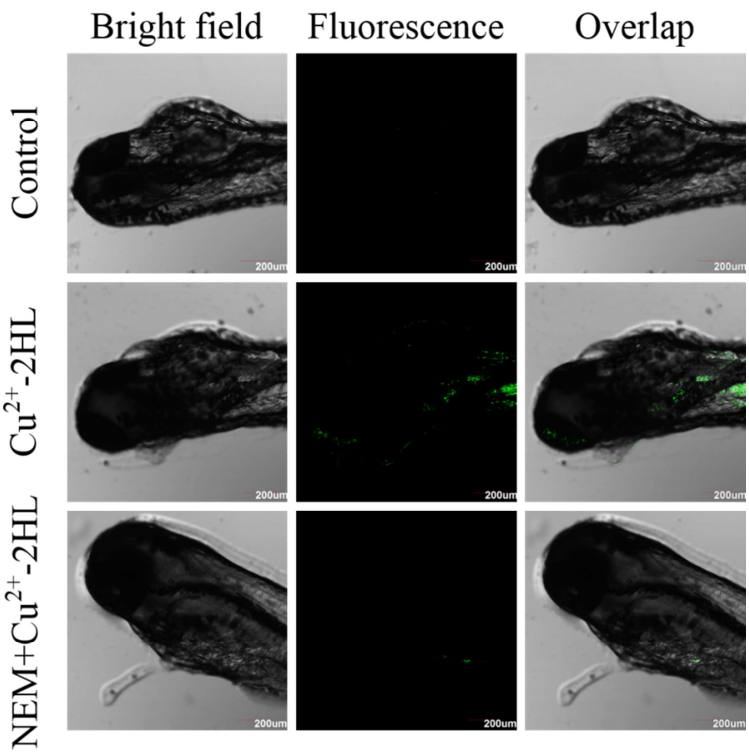

Fig. 11. Fluorescence images of zebrafish larvae incubated with Cu^{2+}-2HL. Bright field image (left), fluorescence image (middle) and overlap image (right). λ_{ex} = 488 nm.

4. Conclusions

A unique chemosensor system for detecting Cu^{2+} and tumor biomarker GSH has been successfully devised, which exhibit high sensitivity, excellent selectivity and good anti-interference over other metal ions or amino acids. The 2:1 binding mode of Cu^{2+} with HL was proven by ESI-MS, IR, Job plots analysis and DFT calculations. The developed chemosensor system shows several significant advantages: (1) simplicity in design and performance; (2) time-saving sensing process in which all the detection is finished within 1 min; (3) can achieve “Naked-eye” detection; (4) can selectively detect GSH in complicated environment including biological interferents HS^-, Hcy and Cys. More importantly, it shows good detection ability in real sample analysis especially for medical diagnosis. Due to its excellent characteristic, this

detection system has great potential for evaluating the tumor biomarker GSH levels in biological and medical fields.

Acknowledgements

This work was supported by National Natural Science Foundation of China (No. 21977080), Tianjin Municipal Natural Science Foundation (No. 17JCZDJC33100, 18JCYBJC89700, 18JCYBJC91300), the Program for Innovative Research Team in University of Tianjin (TD13-5074) and the Science &Technology Development Fund of Tianjin Education Commission for Higher Education (2019ZD15).

References:

[1] Ishida S, Andreux P, Poitry-Yamate C, Auwerx J, Hanahan D. Bioavailable copper modulates oxidative phosphorylation and growth of tumors. Proc. Natl. Acad. Sci. U.S.A. 2013;110:19507–12. https://doi.org/10.1073/pnas.1318431110.

[2] Gupte A, Mumper RJ. Elevated copper and oxidative stress in cancer cells as a target for cancer treatment. Cancer Treat Rev. 2009;35:32–46. https://doi.org/10.1016/j.ctrv.2008.07.004.

[3] Zatta P, Frank A. Copper deficiency and neurological disorders in man and animals. Brain Res. Rev. 2007;54:19–33. https://doi.org/10.1016/j.brainresrev.2006.10.001.

[4] Bull PC, Thomas GR, Rommens JM, Forbes JR, Cox DW. The Wilson disease gene is a putative copper transporting P-type ATPase similar to the menkes gene. Nat. Genet. 1993;5:327–37. https://doi.org/10.1038/ng1293-327.

[5] Hu GF. Copper stimulates proliferation of human endothelial cells under culture. J. Cell. Biochem. 1998;69:326–35. https://doi.org/10.1002/(sici)1097-4644(19980601)69:3<326::aid-jcb10>3.0.co;2-a.

[6] Xie H, Kang YJ. Role of copper in angiogenesis and its medicinal implications. Curr. Med. Chem. 2009;16:1304–14. https://doi.org/10.2174/092986709787846622.

[7] Jung HS, Kwon PS, Lee JW, Kim JI, Hong CS, Kim JW, Yan SH, Lee JY, Lee JH, Joo TH, Kim JS. Coumarin-Derived Cu^{2+}-selective fluorescence sensor: synthesis, mechanisms, and applications in living cells. J. Am. Chem. Soc. 2009;131:2008–12. https://doi.org/10.1021/ja808611d.

[8] Wang CH, Sinskey AJ, Lodish HF. Oxidized redoxstate of glutathione in the endoplasmic reticulum. Science. 1992;257:1496–502. https://doi.org/10.1126/science.1523409.

[9] Guo Q, ZhangY, Lin ZH, Cao QY, ChenY. Fluorescent norbornene for sequential detection of mercury and biothiols. Dyes Pigments 2020;172:107872. https://doi.org/10.1016/j.dyepig.2019.107872.

[10] Meister AJ. Glutathione metabolism and its selective modification. Biol. Chem. 1988;263:17205–8. https://doi.org/10.1111/j.1432-1033.2004.04072.x.

[11] Townsend DM, Tew KD, Tapiero H. The importance of glutathione in human disease. Biomed. Pharmacother. 2003;57:145–55. https://doi.org/10.1016/S0753-3322(03)00043-X.

[12] Li J, Yin CX, Zhang YB, Yue YK, Chao JB, Huo FJ. High selective distinguishable detection GSH and H_2S based on steric configuration of molecular *in Vivo*. Dyes Pigments 2020;172:107826. https://doi.org/10.1016/j.dyepig.2019.107826.

[13] Bui QN, Li Y, Jang MS, Huynh DP, Lee JH, Lee DS. Redox-and pH-sensitive polymeric micelles based on poly(β-amino ester)-grafted disulfide methylene oxide poly(ethylene glycol) for anticancer drug delivery. Macromol. 2015;48:4046–54. https://doi.org/10.1021/acs.macromol.5b00423.

[14] Schnelldorfer T, Gansauge S, Gansauge F, Schlosser S, Beger HG, Nussler AK. Glutathione depletion causes cell growth inhibition and enhanced apoptosis in pancreatic cancer cells. Cancer 2000;89:1440–7. https://doi.org/10.1002/1097-0142(20001001)89:7<1440::AID-CNCR5>3.3.CO;2-S.

[15] Harris IS, Treloar AE, Inoue S, Sasaki M, Gorrini C, Lee KC, Yung KY, Brenner D, Knobbe-Thomsen CB, Cox MA, Elia A, Berger T, Cescon DW, Adeoye A, Brustle A, Molyneux SD, Mason JM, Li WDY, Yamamoto K, Wakeham A, Berman HK, Khokha R, Done SJ, Kavanagh TJ, Lam CW, Mak TW. Glutathione and thioredoxin antioxidant pathways synergize to drive cancer initiation and progression. Cancer Cell. 2015;27:211–22. https://doi.org/10.1016/j.ccell.2014.11.019.

[16] Xiao QF, Zheng XP, Bu WB, Ge WQ, Zhang SJ, Chen F, Xing HY, Ren QG, Fan WP, Zhao KL, Hua YQ, Shi JL. A core/satellite multifunctional nanotheranostic for in vivo imaging and tumor eradication by radiation/photothermal synergistic therapy. J. Am. Chem. Soc. 2013;135:13041–8. https://doi.org/10.1021/ja404985w.

[17] Yuan Z, Gui L, Zheng J, Chen Y, Qu S, Shen Y, Wang F, Er M, Gu Y, Chen H. GSH-activated light-up near-infrared fluorescent probe with high affinity to $\alpha_v\beta_3$ integrin for precise early tumor identification. ACS Appl. Mater. Interfaces 2018;10:30994−1007. https://doi.org/10.1021/acsami.8b09841.

[18] Wu SY, Min H, Shi W, Cheng P. Multicenter metal-organic framework-based ratiometric fluorescent sensors. Adv. Mater. 2019;31:1805871. https://doi.org/10.1002/adma.201805871.

[19] Qian XH, Xu ZC. Fluorescence imaging of metal ions implicated in diseases. Chem. Soc. Rev. 2015;44:4487−93. https://doi.org/10.1039/c4cs00292j.

[20] Zhao B, Chen XY, Cheng P, Liao DZ, Yan SP, Jiang ZH. Coordination polymers containing 1D channels as selective luminescent probes. J. Am. Chem. Soc. 2004;126:15394−95. https://doi.org/10.1021/ja047141b.

[21] Zhou JM, Li HH, Zhang H, Li HM, Shi W, Cheng P. A bimetallic lanthanide metal-organic material as a self-calibrating color-gradient luminescent sensor. Adv. Mater. 2015;27:7072−7. https://doi.org/10.1002/adma.201502760.

[22] Zhang SY, Shi W, Cheng P, Zaworotko MJ. A mixed-crystal lanthanide zeolite-like metal-organic framework as a fluorescent indicator for lysophosphatidic acid, a cancer biomarker. J. Am. Chem. Soc. 2015;137:12203−6. https://doi.org/10.1021/jacs.5b06929.

[23] Lee S, Li J, Zhou X, Yin J, Yoon J. Recent progress on the development of glutathione (GSH) selective fluorescent and colorimetric probes. Coord. Chem. Rev. 2018;366:29–68. https://doi.org/10.1016/j.ccr.2018.03.021.

[24] Hu ZQ, Sun LL, Gu YY, Jiang Y. A sensitive and selective fluorescent probe for detection of glutathione in the presence of Cu^{2+} and its application to biological imaging. Sens. Actuators B-Chem. 2015;212:220–4. https://doi.org/10.1016/j.snb.2015.01.084.

[25] Liu Y, Duan Y, Gill AD, Perez L, Jiang Q, Hooley RJ, Zhong W. Metal-assisted selective recognition of biothiols by a synthetic receptor array. Chem. Commun. 2018;54:13147–50. https://doi.org/10.1039/c8cc07220e.

[26] Hu Y, Heo CH, Kim G, Jun EJ, Yin J, Kim HM, Yoon J. One-photon and two-photon sensing of biothiols using a bis-pyrene-Cu(II) ensemble and its application to image GSH in the cells and tissues. Anal. Chem. 2015;87:3308–13. https://doi.org/10.1021/ac504372w.

[27] Jiao Y, Zhou L, He HY, Yin JQ, Duan CY. A new fluorescent chemosensor for recognition of Hg^{2+} ions based on a coumarin derivative. Talanta 2017;162:403–7. https://doi.org/10.1016/j.talanta.2016.10.004.

[28] Li N, Xiang Y, Tong AJ. Highly sensitive and selective “turn-on” fluorescent chemodosimeter for Cu^{2+} in water via Cu^{2+}-promoted hydrolysis of lactonemoiety in coumarin. Chem. Commun. 2010;46:3363–5. https://doi.org/10.1039/c001408g.

[29] Zhang Y, Guo XF, Tian XJ, Liu AD, Jia LH. Carboxamidoquinoline-coumarin derivative: a ratiometricfluorescent sensorfor Cu(II) in a dual fluorophore hybrid. Sens. Actuators B-Chem. 2015;218:37–41. https://doi.org/10.1016/j.snb.2015.04.100.

[30] Liao YC, Venkatesan P, Wei LF, Wu SP. A coumarin-based fluorescent probe for thiols and its application in cell imaging. Sens. Actuators B-Chem. 2016;232:732–7. https://doi.org/10.1016/j.snb.2016.04.027.

[31] Liu YJ, Tian FF, Fan XY, Jiang FL, Liu Y. Fabrication of an acylhydrazone based fluorescence probe for Al^{3+}. Sens. Actuators B-Chem. 2017;240:916–25. https://doi.org/10.1016/j.snb.2016.09.051.

[32] Dhara A, Guchhait N, Mukherjee I, Mukherjee A, Bhattacharya SC. A novel pyrazole based single molecular probe for multi-analyte (Zn^{2+} and Mg^{2+}) detection in human gastric adenocarcinoma cells. RSC Adv. 2016;6:105930–9. https://doi.org/10.1039/c6ra22869k.

[33] Wang ZG, Wang Y, Ding XJ, Sun YX, Xie CZ, Qian J, Li QZ, Xu JY. A highly selective colorimetric and fluorescent probe for quantitative detection of Cu^{2+}/Co^{2+}: the unique ON-OFF-ON fluorimetric detection strategy and applications in living cells/zebrafish. Spectrochim. Acta A In Press. https://doi.org/10.1016/j.saa.2019.117763

[34] Wang Y, Ma ZY, Zhang DL, Deng JL, Chen X, Xie CZ, Qiao X, Li QZ, Xu JY. Highly selective and sensitive turn-on fluorescent sensor for detection of Al^{3+} based on quinoline-base Schiff base. Spectrochim. Acta A 2018;195:157–64. https://doi.org/10.1016/j.saa.2018.01.049.

[35] Wang Y, Wang ZG, Song XQ, Chen Q, Tian H, Xie CZ, Li QZ, Xu JY. Dual functional turn-on non-toxic chemosensor for highly selective and sensitive visual

detection of Mg^{2+} and Zn^{2+}: solvent-controlled recognition effect and bio-imaging application. Analyst 2019;144:4024–32. https://doi.org/10.1039/c9an00583h.

[36] Xu W, Han GJ, Ma PY, Diao QP, Xu LB, Liu X, Sun Y, Wang XH, Song DQ. A highly selective turn-on fluorescent and chromogenic probe for CN^- and its applications in imaging of living cells and zebrafish in vivo. Sens. Actuators B-Chem. 2017;251:366–73. https://doi.org/10.1016/j.snb.2017.05.088.

[37] Mergu N, Kim M, Son YA. A coumarin-derived Cu^{2+}-flluorescent chemosensor and its direct application in aqueous media. Spectrochim. Acta A 2018;188:571–80. https://doi.org/10.1016/j.saa.2017.07.047.

[38] Wang Y, Mao PD, Wu WN, Mao XJ, Fan YC, Zhao XL, Xu ZQ, Xu ZH. New pyrrole-based single-molecule multianalyte sensor for Cu^{2+}, Zn^{2+}, and Hg^{2+} and its AIE activity. Sens. Actuators B-Chem. 2018;255:3085–92. https://doi.org/10.1016/j.snb.2017.09.133.

[39] Li KB, Jia WP, Han DM, Liang DX, He XP, Chen GR. Fluorogenic bis-triazolyl galactoprobe-metal complex for full-aqueous analysis of sulfide ion. Sens. Actuators B-Chem. 2017;246:197–201. https://doi.org/ 10.1016/j.snb.2017.02.082.

[40] Wu SY, Lin YN, Liu JW, Shi W, Yang GM, Cheng P. Rapid detection of the biomarkers for carcinoid tumors by a water stable luminescent lanthanide metal-organic framework. Adv. Funct. Mater. 2018;28:1707169. https://doi.org/10.1002/adfm.201707169.

[41] Hao JN, Yan B. Determination of urinary 1-hydroxypyrene for biomonitoring of human exposure to polycyclic aromatic hydrocarbons carcinogens by a

lanthanide-functionalized metal-organic framework. Adv. Funct. Mater. 2017;27:1603856. https://doi.org/10.1002/adfm.201603856.

[42] Ding L, Wang S, Liu Y, Cao J, Fang Y. Bispyrene/surfactant assemblies as fluorescent sensor platform: detection and identification of Cu^{2+} and Co^{2+} in aqueous solution. J. Mater. Chem. A. 2013;1: 8866–75. https://doi.org/ 10.1039/c3ta10453b.

[43] Frisch MJ, Trucks GW, Schlegel HB, Scuseria GE, Robb MA, Cheeseman JR, et al. Gaussian 09 (Revision A. 1), Gaussian, Inc, Wallingford, CT. (2009).

[44] Liu ZC, Wang BD, Li B, Wang Q, Yang ZY, Li TR, Li Y. Crystal structures, DNA-binding and cytotoxic activities studies of Cu(II) complexes with 2-oxo-quinoline-3-carbaldehyde Schiff-bases. Eur. J. Med. Chem. 2010;45:5353–61. https://doi.org/10.1016/j.ejmech.2010.08.060.

[45] Shit S, Dey SK, Rizzoli C, Zangrando E, Pilete G, Gómez-García CJ, Mitra S. The key role of hydrogen bonding in the nuclearity of three copper(II) complexes with hydrazone-derived ligands and nitrogen donor heterocycles. Inorg. Chim. Acta. 2011;15:18–26. https://doi.org/10.1016/j.ica.2011.01.008.

[46] Umezawa K, Yoshida M, Kamiya M, Yamasoba T, Urano Y. Rational design of reversible fluorescent probes for live-cell imaging and quantification of fast glutathione dynamics. Nat. Chem. 2017;9:279–86. https://doi.org/10.1038/nchem.2648.

[47] Zhao H, Wen X, Li W, Li Y, Yin C. Copper-mediated On-Off-On gold nanocluster for endogenous GSH sensing to drive cancer cell recognition. J. Mater. Chem. B 2019;7:2169–76. https://doi.org/10.1039/C8TB03184C.

[48] Fishman MC. Genomics. Zebrafish–the canonical vertebrate. Science 2001;294:1290−1. https://doi.org/10.1126/science.1066652.

[49] Milan DJ, Peterson TA, Ruskin JN, Peterson RT, MacRae CA. Drugs that induce repolarization abnormalities cause bradycardia in zebrafish. Circulation 2003;107:1355−8. https://doi.org/10.1161/01.cir.0000061912.88753.87.

- New chemosensor for colorimetric and fluorescent detection of Cu^{2+} and GSH.
- The probe displays high selectivity, excellent sensitivity and short response time.
- Fast recognition of Cu^{2+} and GSH can be achieved by naked eye.
- Detecting endogenous and exogenous glutathione in living cells and zebrafish.
- Cancer identification was achieved by endogenous GSH sensing.

Declaration of interests

☒ The authors declare that they have no known competing financial interests or personal relationships that could have appeared to influence the work reported in this paper.

☐The authors declare the following financial interests/personal relationships which may be considered as potential competing interests: